Sharp bends and Mach-Zehnder interferometer based on Ge-rich-SiGe waveguides on SiGe graded buffer

Vladyslav Vakarin,[1] Papichaya Chaisakul,[1,2] Jacopo Frigerio,[3] Andrea Ballabio,[3] Xavier Le Roux,[1] Jean-René Coudevylle,[1] David Bouville,[1] Diego Perez-Galacho,[1] Laurent Vivien,[1] Giovanni Isella,[3] and Delphine Marris-Morini[1,*]

[1] *Institut d'Electronique Fondamentale, Univ. Paris-Sud, CNRS, Univ. Paris-Saclay, UMR 8622, Bât. 220, 91405 Orsay Cedex, France*

[2] *Department of Materials Engineering, The University of Tokyo, 7-3-1 Hongo, Bunkyo-Ku, Tokyo, 113-8656, Japan*

[3] *L-NESS, Dipartimento di Fisica, Politecnico di Milano, Polo di Como, Via Anzani 42, I 22100 Como, Italy*

[*] *delphine.morini@u-psud.fr*

Abstract: The integration of germanium (Ge)-rich active devices in photonic integrated circuits is challenging due to the lattice mismatch between silicon (Si) and Ge. A new Ge-rich silicon-germanium (SiGe) waveguide on graded buffer was investigated as a platform for integrated photonic circuits. At a wavelength of 1550 nm, low loss bends with radii as low as 12 µm and Multimode Interferometer beam splitter based on Ge-rich SiGe waveguide on graded buffer were designed, fabricated and characterized. A Mach Zehnder interferometer exhibiting a contrast of more than 10 dB has been demonstrated.

OCIS codes: (230.0230) Optical devices; (230.7370) Waveguides.

References and links

1. R. Koerner, M. Oehme, M. Gollhofer, M. Schmid, K. Kostecki, S. Bechler, D. Widmann, E. Kasper, and J. Schulze, "Electrically pumped lasing from Ge Fabry-Perot resonators on Si," Opt. Express **23**(11), 14815–14822 (2015).
2. R. E. Camacho-Aguilera, Y. Cai, N. Patel, J. T. Bessette, M. Romagnoli, L. C. Kimerling, and J. Michel, "An electrically pumped germanium laser," Opt. Express **20**(10), 11316–11320 (2012).
3. A. V. Krishnamoorthy, X. Zheng, D. Feng, J. Lexau, J. F. Buckwalter, H. D. Thacker, F. Liu, Y. Luo, E. Chang, P. Amberg, I. Shubin, S. S. Djordjevic, J. H. Lee, S. Lin, H. Liang, A. Abed, R. Shafiiha, K. Raj, R. Ho, M. Asghari, and J. E. Cunningham, "A low-power, high-speed, 9-channel germanium-silicon electro-absorption modulator array integrated with digital CMOS driver and wavelength multiplexer," Opt. Express **22**(10), 12289–12295 (2014).
4. P. Chaisakul, D. Marris-Morini, M. S. Rouifed, G. Isella, D. Chrastina, J. Frigerio, X. Le Roux, S. Edmond, J.-R. Coudevylle, and L. Vivien, "23 GHz Ge/SiGe multiple quantum well electro-absorption modulator," Opt. Express **20**(3), 3219–3224 (2012).
5. J. Liu, M. Beals, A. Pomerene, S. Bernardis, R. Sun, J. Cheng, L. C. Kimerling, and J. Michel, "Waveguide integrated, ultra-low energy GeSi electro-absorption modulators," Nat. Photonics **2**(7), 433–437 (2008).
6. L. Virot, P. Crozat, J.-M. Fédéli, J.-M. Hartmann, D. Marris-Morini, E. Cassan, F. Boeuf, and L. Vivien, "Germanium avalanche receiver for low power interconnects," Nat. Commun. **5**, 4957 (2014).
7. H. T. Chen, P. Verheyen, P. De Heyn, G. Lepage, J. De Coster, P. Absil, G. Roelkens, and J. Van Campenhout, "High-responsivity low-voltage 28-Gb/s p-i-n photodectector with silicon contacts," J. Lightwave Technol. **33**(4), 820–824 (2015).
8. P. Chaisakul, D. Marris-Morini, J. Frigerio, D. Chrastina, M. S. Rouifed, S. Cecchi, P. Crozat, G. Isella, and L. Vivien, "Integrated germanium optical interconnects on silicon substrates," Nat. Photonics **8**(6), 482–488 (2014).
9. Y.-H. Kuo, Y. K. Lee, Y. Ge, S. Ren, J. E. Roth, T. I. Kamins, D. A. Miller, and J. S. Harris, "Strong quantum-confined Stark effect in germanium quantum-well structures on silicon," Nature **437**(7063), 1334–1336 (2005).
10. M.-S. Rouifed, D. Marris-Morini, P. Chaisakul, J. Frigerio, G. Isella, D. Chrastina, S. Edmond, X. Le Roux, J.-R. Coudevylle, D. Bouville, and L. Vivien, "Advances toward Ge/SiGe quantum-well waveguide modulators at 1.3µm," IEEE J. Sel. Top. Quantum Electron. **20**(4), 33 (2014).
11. L. Lever, Y. Hu, M. Myronov, X. Liu, N. Owens, F. Y. Gardes, I. P. Marko, S. J. Sweeney, Z. Ikonić, D. R. Leadley, G. T. Reed, and R. W. Kelsall, "Modulation of the absorption coefficient at 1.3 µm in Ge/SiGe multiple quantum well heterostructures on silicon," Opt. Lett. **36**(21), 4158–4160 (2011).

#250423 Received 21 Sep 2015; accepted 23 Oct 2015; published 17 Nov 2015

12. J. Liu, "Monolithically integrated Ge-on-Si active photonics," Photonics **1**(3), 162–197 (2014).
13. C. G. Littlejohns, M. Nedeljkovic, C. F. Mallinson, J. F. Watts, G. Z. Mashanovich, G. T. Reed, and F. Y. Gardes, "Next generation device grade silicon-germanium on insulator," Sci. Rep. **5**, 8288 (2015).
14. K. Hammani, M. A. Ettabib, A. Bogris, A. Kapsalis, D. Syvridis, M. Brun, P. Labeye, S. Nicoletti, D. J. Richardson, and P. Petropoulos, "Optical properties of silicon germanium waveguides at telecommunication wavelengths," Opt. Express **21**(14), 16690–16701 (2013).
15. S. F. Pesarcik, G. V. Treyz, S. S. Iyer, and J. M. Halbout, "Silicon germanium optical waveguides with 0.5 dB/cm losses for singlemode fibre optic systems," Electron. Lett. **28**(2), 159–160 (1992).
16. S. P. Pogossian, L. Vescan, and A. Vonsovici, "High-confinement SiGe low-loss waveguides for Si-based optoelectronics," Appl. Phys. Lett. **75**(10), 1440 (1999).
17. J. Frigerio, P. Chaisakul, D. Marris-Morini, S. Cecchi, M. S. Roufied, G. Isella, and L. Vivien, "Electro-refractive effect in Ge/SiGe multiple quantum wells," Appl. Phys. Lett. **102**(6), 061102 (2013).
18. K. Popovic, K. Wada, S. Akiyama, H. A. Haus, and J. Michel, "Air trenches for sharp silica waveguide bends," J. Lightwave Technol. **20**(9), 1762–1772 (2002).
19. L. H. Spiekman, Y. S. Oei, E. G. Metaal, F. H. Groen, P. Demeester, and M. K. Smit, "Ultrasmall waveguide bends: the corner mirrors of the future?" IEE Proc., Optoelectron. **142**(1), 61–65 (1995).
20. T. Kitoh, N. Takato, M. Yasu, and M. Kawachi, "Bending loss reduction in silica-based waveguides by using lateral offsets," J. Lightwave Technol. **13**(4), 555–562 (1995).
21. M. Cherchi, S. Ylinen, M. Harjanne, M. Kapulainen, and T. Aalto, "Dramatic size reduction of waveguide bends on a micron-scale silicon photonic platform," Opt. Express **21**(15), 17814–17823 (2013).

1. Introduction

On-Chip optical interconnects are a promising option to overcome the limitations of electrical interconnects such as the high power consumption and limited bandwidth. Germanium (Ge) is considered as a material of choice for the development of efficient and reliable photonic circuits integrated on silicon (Si), due to its pseudo-direct gap properties and its compatibility with mature Si technology. Ge has been investigated for many photonic devices such as light sources [1,2], modulators [3–5] and photodetectors [6,7]. Specific techniques have been reported to accommodate the lattice mismatch between Si and Ge or silicon-germanium (SiGe) such as the use of high temperature thermal annealing (typically more than 800°C) to reduce threading dislocations [1,5,6], or the use of relaxed buffers including (i) linearly graded buffer [8], (ii) thin SiGe layers [9,10] and (iii) reverse graded structures [11]. It can be noted that other techniques have been explored recently, based on the growth of crystalline Ge on amorphous Si [12] or silicon-germanium on insulator using a rapid melt growth technique [13]. From the photonic integration's point of view, the combination of active devices with efficient and low loss waveguides and passive structures is also of major importance. The integration of active Ge optoelectronics with the silicon-on-insulator (SOI) waveguides has been the most common approach so far [1–3,5–7]. Alternatively it was shown in [8] that virtual substrates (VS) on linearly graded buffer can act as an optical waveguide, on which low temperature (< 450°C) and high quality epitaxial growth of Ge rich layers can be carried out. An optical interconnect link including an electro-absorption modulator and a photodector based on Ge/SiGe quantum wells (QW) heterostructures connected by a passive Ge-rich SiGe waveguide grown on bulk Si wafer was shown.

Low-loss $Si_{1-x}Ge_x$ waveguides have also been reported previously with a low Ge content x between 0.01 and 0.3 [14–16] in order to avoid high dislocation defects density between Si substrate and $Si_{1-x}Ge_x$ waveguide. However in these cases, the large lattice mismatch that would occur between the SiGe waveguide and Ge-rich active devices makes unlikely a straightforward integration between waveguides and active devices, from the epitaxy viewpoint. In comparison, the Ge content of $Si_{1-x}Ge_x$ waveguide on graded buffer used in [8] was larger than 0.8, allowing the integration with Ge photonic devices; however, only straight waveguides were demonstrated as a first proof of concept, and compact optical guiding structures remained questionable owning to the low refractive index contrast between the waveguide core and the graded buffer.

Moreover, a strong electro-refraction [17] has been recently demonstrated in Ge/SiGe QW. This effect could be used to achieve optical modulation but requires the embedding of the QWs in a Mach-Zehnder interferometer.

#250423 Received 21 Sep 2015; accepted 23 Oct 2015; published 17 Nov 2015

In this context, this paper experimentally demonstrates the possibility to use the new Ge-rich SiGe on graded buffer waveguide as a promising platform for photonic integration: sharp bends and an integrated Mach-Zehnder interferometer including SiGe waveguides and a compact beam splitter were demonstrated from Ge-rich SiGe waveguide on graded buffer. These results pave the way toward the monolithic integration of Ge-based active devices with efficient and compact passive Ge-rich SiGe optical circuitry on bulk silicon wafers.

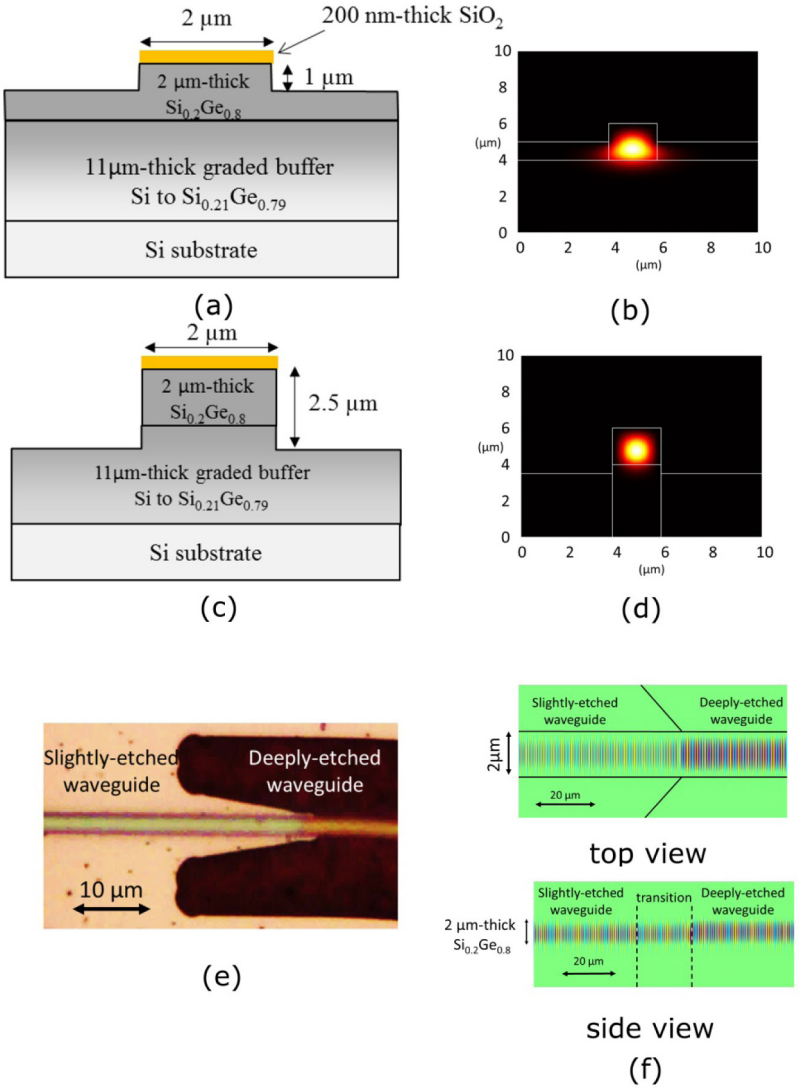

Fig. 1. (a) Schematic cross section of the slightly-etched $Si_{0.2}Ge_{0.8}$ waveguide on graded buffer, (b) corresponding optical mode (TE-polarization), (c) schematic cross section of the deeply-etched $Si_{0.2}Ge_{0.8}$ waveguide, (d) corresponding optical mode (TE-polarization), (e) optical microscope view of the transition between a slightly-etched and a deeply-etched waveguide to increase the light confinement at the bends (deeply-etched regions appear darker), (f) numerical simulation of light propagation (TE polarization) along the transition, calculated by eigenmode expansion solver.

#250423 Received 21 Sep 2015; accepted 23 Oct 2015; published 17 Nov 2015

2. Experimental results and discussion

The SiGe waveguide on graded buffer used as the preliminary building block in this work is shown in Fig. 1(a). This waveguide led to a single mode propagation in TE-polarization according to optical mode calculation (Fig. 1(b)), and confirmed by infrared camera inspection at the output waveguide. Light is vertically confined in a 2µm-thick relaxed $Si_{0.2}Ge_{0.8}$ layer on top of a $Si_{1-x}Ge_x$ graded buffer. The Ge concentration x of the graded buffer is linearly increased from 0 to 0.79 over a thickness of 11µm. The refractive index variation is then varied from 3.477 to 4.112 at a wavelength of 1.55 µm as obtained by linearly interpolating the refractive index of Si and Ge.

Low energy plasma enhanced chemical vapor deposition (LEPECVD) was used for the growth of the SiGe stack. Rib waveguides were then defined for lateral confinement. A 200nm-thick SiO_2 layer was deposited on $Si_{0.2}Ge_{0.8}$ to act as a hard mask. SiO_2 was first patterned using deep UV lithography followed by reactive ion etching (RIE). Waveguides were then etched using Inductively Coupled Plasma (ICP) etching. The etching depth was only 1µm in the straight portions of the waveguide to limit the influence of sidewall roughness. To reduce the curvature radius of bent waveguides, a deeper etch of of the waveguides was performed to increase the mode confinement and then define sharper bends (Figs. 1(c) and 1(d)) [18, 19]. The hard mask was used to self-align the second etching step with the patterned waveguides. The total etching depth of the deeply-etched waveguide was 2.5 µm. The transition between both straight and bent waveguides is shown in Fig. 1(e). The deeply-etched regions appear darker, on both sides of the waveguide. The 20-µm-long taper section was used to avoid an abrupt change in the effective index between the slightly- and deeply-etched sections, and maintains a compact footprint of the overall bending section (including the taper region). A numerical simulation of light propagation along the transition calculated by an eigenmode expansion solver is reported in Fig. 1(f). A slice located 1µm below the top of the waveguide is considered for the top view calculation while a slice in the middle of the waveguide is used for the side view calculation. From this calculation no radiation losses is seen which indicates a good design of the transition between both waveguides.

Optical losses were evaluated comparing the transmission of the straight waveguides and a set of waveguides including 32 consecutive bends to obtain reliable bending loss data. 12, 25, 50 and 100 µm bend radii have been compared. A view of the bending test structure is shown in Figs. 2(a) and 2(b).

The measurements were performed at 1.55µm, i.e. above the indirect optical absorption band-edge of $Si_{0.2}Ge_{0.8}$. TE-polarized light was butt-coupled into the waveguides using a lensed fiber. An objective was used at the output to inject the light in a photodetector. Optical losses of straight waveguides (cut section of Fig. 1(a)) were estimated to be 1 dB/mm. These losses can be further reduced, by decreasing the sidewall roughness by etching process optimization and /or by improving surface passivation, down to typically 2dB/cm which has been measured previously [8].

The losses of the 90° bends are reported in Fig. 2(c). Optical losses increase for sharper bend radii. 0.5 dB/90° bend was obtained for a 50µm radius. Numerical simulations indicate that the main contribution of the losses is the modal mismatch between the straight and the bent waveguide. Bending loss could thus be further reduced to typically 0.1dB/90° using an offset technique [20] or using bend shapes with continuously varying curvature [21] to decrease the modal mismatch.

Mach Zehnder interferometers based on SiGe waveguides have also been investigated. In most photonics circuit applications, the ability to measure and manipulate the phase of one wave with respect to another is essential; therefore, an interferometer can be considered fundamental in proving the validity of a new photonic platform. First, Multi-Mode interferometer (MMI) splitters based on the waveguide reported in Fig. 1(a) have been

#250423 Received 21 Sep 2015; accepted 23 Oct 2015; published 17 Nov 2015

designed. Figure 3 presents the geometry of the optimized structure as well as the simulation. A 187µm-long MMI splitter was used, with 3.5 µm-wide output waveguides, separated by 2.3µm.

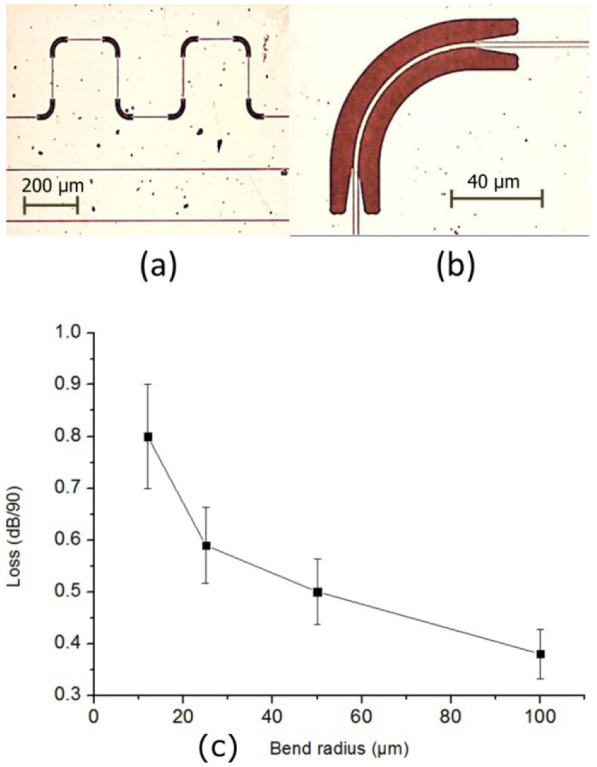

Fig. 2. (a) Optical microscope view of the bending test structure (b), zoom of the 90° bend and its deeply-etched region, (c) Measured losses of the 90° bends as function of bend radius

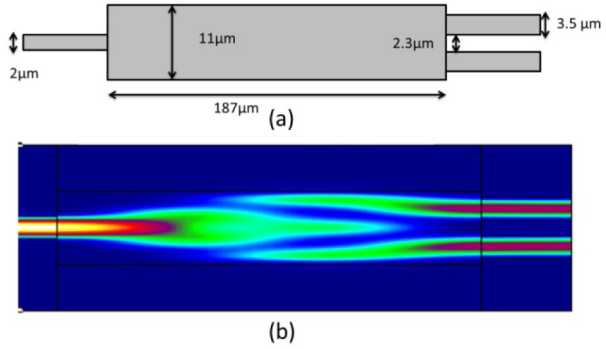

Fig. 3. MMI Beam splitter: (a) Schematic view of the device, (b) Propagation simulation of the electric field component (waveguide cross section is in Fig. 1(b))

Asymmetric Mach-Zehnder interferometers have thus been fabricated and characterized. The general view of the Mach-Zehnder interferometer is shown in Fig. 4(a), including the designed MMI splitter (Fig. 4(b)). The bending region of the interferometer have been deeply etched as can be seen in Fig. 4(c). The transmission of the Mach Zehdner is reported in Fig. 4(d). A free spectral range of 24.4 nm is obtained which is in good agreement with a length difference of 24 µm between both arms of the interferometer. 12 dB losses are estimated

#250423 Received 21 Sep 2015; accepted 23 Oct 2015; published 17 Nov 2015

between the input and output of the chip including 2 dB waveguide loss in the 2 mm-long Mach Zehnder arms, 1 dB loss for each coupler, and 8 dB waveguide loss in the 8 mm-long input and output access waveguide which could be dramatically reduced by decreasing the length of access waveguides. Significantly, the extinction higher than 10 dB indicated the good balance of the couplers.

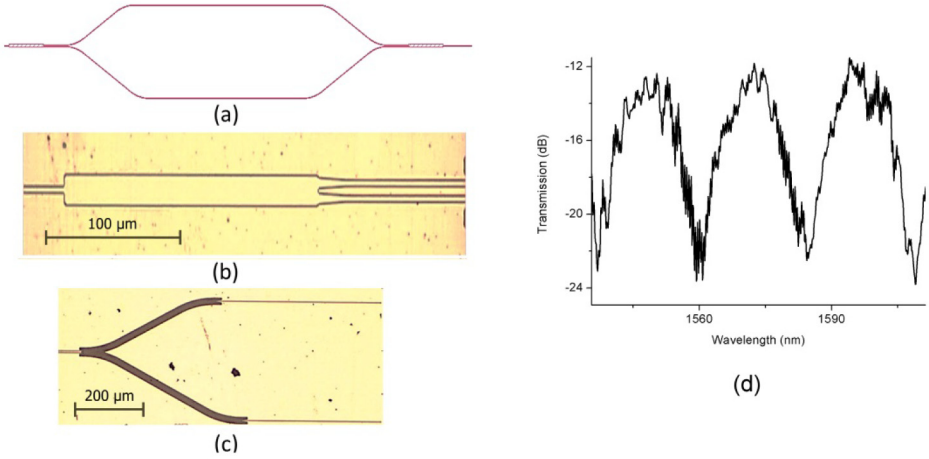

Fig. 4. Asymmetric Mach Zehnder: (a) general schematic view, (b) optical microscope view of the MMI, (c) optical microscope view of the waveguide separation after the MMI, (d) Optical transmission as a function of the wavelength. The free spectral range of 24.4 nm is related to the length difference of 24 µm between both arms of the Mach-Zehnder

3. Conclusion

In conclusion, Ge-rich SiGe waveguides on graded buffer open a new possibility to integrate Ge-based active and passive photonics components through innovative band-gap (refractive index) engineering, while the use of such a graded buffer allows a high quality Ge-rich $Si_{1-x}Ge_x$ layer on Si. This material platform allows the fabrication of the main building blocks for passive waveguide devices. Low propagation loss, compact 90° turns and good extinction ratio Mach Zehnder interferometer have been experimentally validated. Different light confinements have been used to ensure an appropriate mode confinement in Ge-rich SiGe structures. The fabrication was based on a self-aligned two etching process to achieve a perfect alignment and then reduce the loss in the slightly/deeply-etched waveguides transition. This work paves the way for the demonstration of wavelength division multiplexing devices and their integration with active devices (sources, modulators and photodectectors) and in consequence to go towards SiGe-based photonic integrated transceivers on bulk silicon substrate.

Acknowledgments

The CARIPLO foundation is acknowledged for financial support through the grant EIDOS 2011-038. The fabrication of the device was performed at the nano-center CTU-IEF-Minerve, which is partially funded by the "Conseil Général de l'Essonne". This work was partly supported by the French RENATECH network. D.M-M. acknowledges support by the Institut Universitaire de France. Marie Curie International Outgoing Fellowships through grant agreement PIOF-GA-2013-629292 MIDEX is partly acknowledged. This project has received funding from the European Research Council (ERC) under the European Union's Horizon 2020 research and innovation programme (grant agreement N°639107-INsPIRE).